CORNING GLASS WORKS
ELECTRO-OPTICS LABORATORY
RALEIGH, NORTH CAROLINA

IMPROVED SCREEN FOR REAR PROJECTION VIEWERS

Technical Report No. - 14

Date - October 12, 1966

Period Covered - September 16, 1966
to
October 12, 1966

[redacted]

[redacted]

25X1

ABSTRACT

This report summarizes the light scattering properties of additional samples of Corning Glass Works materials. Good agreement was found between the experimental and theoretical data on the fraction of the incident energy scattered into $\pm 45^{\circ}$ and into $\pm 90^{\circ}$. Some samples were found to have excessive particle densities and new samples of these materials will be prepared.

The samples of Fotoform® glass with the surface layer of crystalline material were found to have good, easily controllable optical properties which include low sensitivity to ambient light. Samples of lenticular screens were fabricated using small glass beads. This work is discussed along with the status of the lenticular ribbon which is being re-drawn.

The complete modulation transfer function analyzer is shown along with a discussion of its basic construction.

TECHNICAL REPORT #14

I. Materials Investigations

A. Glass-Ceramics

As part of our continuing effort to identify new and promising materials we have obtained additional samples of glass-ceramic materials. These have been evaluated and the results are summarized in Table I. Data concerning the angular gain function and other optical parameters are given in the Data Appendix.

The diffuse transmittance as a function of axial gain, which is a good measure of the efficiency of a material, is plotted in Figure 1. The fraction of power within $\pm 45^{\circ}$ as a function of axial gain is shown in Figure 2. As before, we see that our materials fall close to the theoretically predicted curve*. Samples AG1, AG2, AG3, and AH1 look very poor both from the angular gain data and from their low values of T_s due to the high concentration of scattering particles. We are requesting additional melts of these glasses with lower particle concentrations. Samples AH1A and AH1B should have had excellent color fidelity as the relative index of refraction between the crystals and the surrounding glass is .65. Sample AC18C was cut from the same block of material as AC18A and AC18B, and AC19C and AC19D were cut from the same material as AC19A and AC19B, which are the two best glass-ceramic materials found thus far.

Figure 3 shows how diffuse transmittance varies with sample thickness. The large variations in T_s occur primarily because the samples are not completely uniform as could be seen from pieces of the original material. We are making an effort to have more homogeneous samples in the future.

Samples AG4A and AG4B look promising from their angular gain curves and from T_{spec}; however, both show some slight red transmission and, when used in a rear projection configuration, the filament of the projection lamp can easily be seen. The remaining samples show small

[redacted] "Improved Screen for Rear Projection Viewers", Technical Report No. 12, August 24, 1966. 25X1

Table I. Summary of Optical Properties

Sample Code	T_s %	T_{45} %	T_{spec} %	Axial Gain	Half Gain Point (°)	Brightness Variation Within ±45° (±%)	Thickness MM
				Glass Ceramics			
AC-18C	66.	25.	0.0	1.7	81.8	3.57	0.533
AC-19C	44.	16.	0.0	1.1	81.4	2.52	1.050
AC-19D	62.	23.	0.0	1.7	80.5	4.75	0.572
AG-1A	34.	12.	0.0	0.9	80.0	1.40	0.584
AG-1B	38.	14.	0.0	1.0	80.0	2.56	1.016
AG-2A	24.	8.6	0.0	0.6	81.0	0.08	0.584
AG-3A	25.	9.2	0.0	0.7	80.5	3.38	0.584
AG-4A	66.	25.	0.0	2.1	78.0	12.6	1.016
AG-4B	81.	34.	0.2	3.5	55.0	29.2	0.559
AH-1A	40.	15.	0.0	1.0	80.0	1.53	0.965
AH-1B	58.	22.	0.0	1.5	74.0	1.75	0.467
AI-1A	62.	24.	0.23	1.7	79.0	4.61	1.074
AI-1B	34.	12.	1.47	0.9	81.0	6.88	0.559
AI-2A	32.	12.	0.0	0.8	81.3	0.99	1.016
AI-2B	42.	16.	0.0	1.1	80.9	3.58	0.546
				Fotoform ® Glass			
AD-15	94.	71.	0.0	113.0	5.5	98.5	0.106
AD-17	88.	43.	0.0	7.1	19.0	55.3	0.168
AD-19	80.	33.	0.0	2.4	77.5	9.86	0.322
AD-21	92.	44.	0.0	4.1	52.5	27.9	0.286
				Commercial Screen Material			
TR-80G	91.	80.		27.0	14.6	92.3	
LS-40-120	93.	50.		6.4	31.0	49.3	
LS-60-120	68.	40.		6.8	21.8	64.1	
OC-70FM	92.	61.		20.0	12.0	84.4	

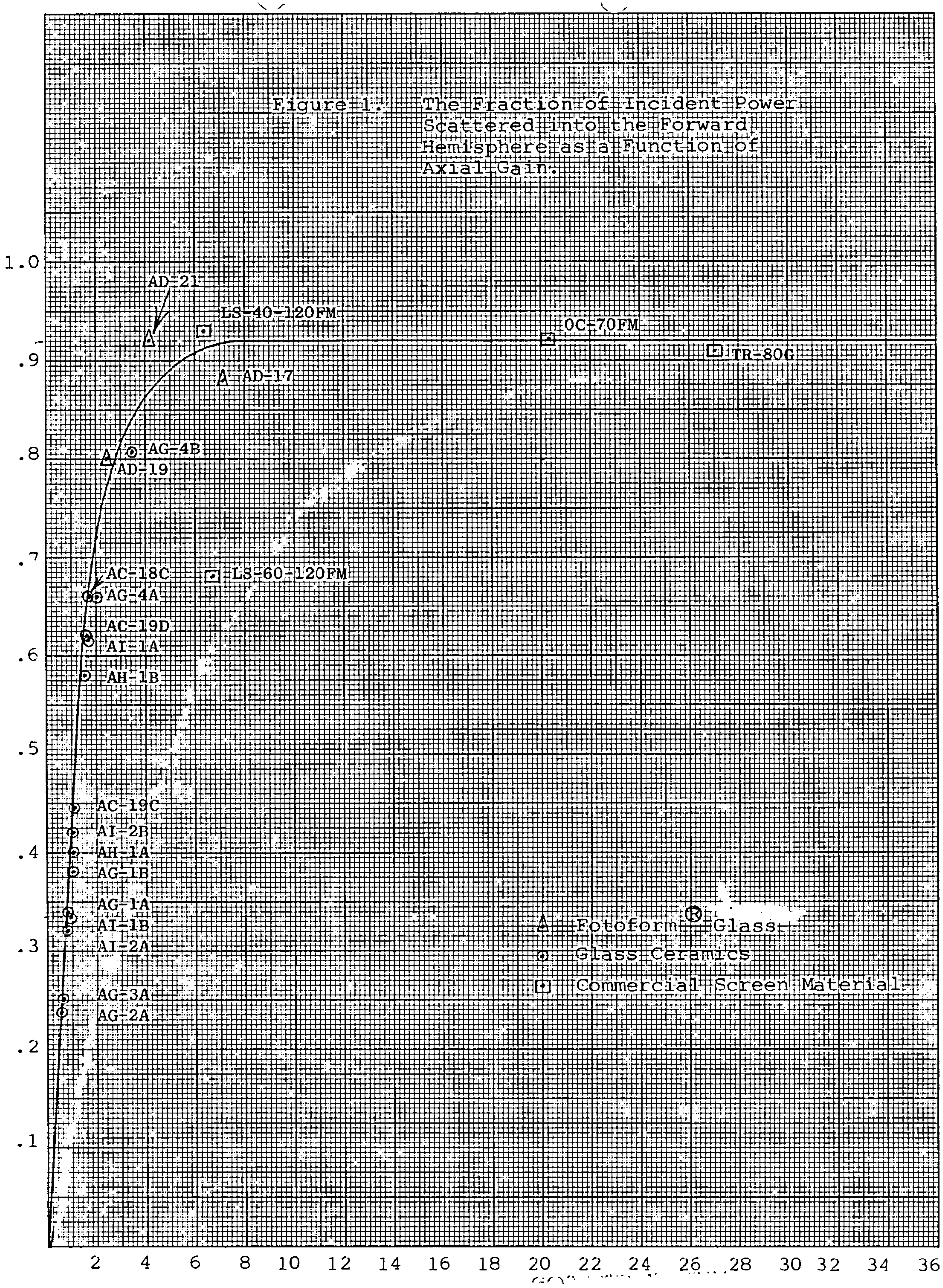

Figure 1. The Fraction of Incident Power Scattered into the Forward Hemisphere as a Function of Axial Gain.

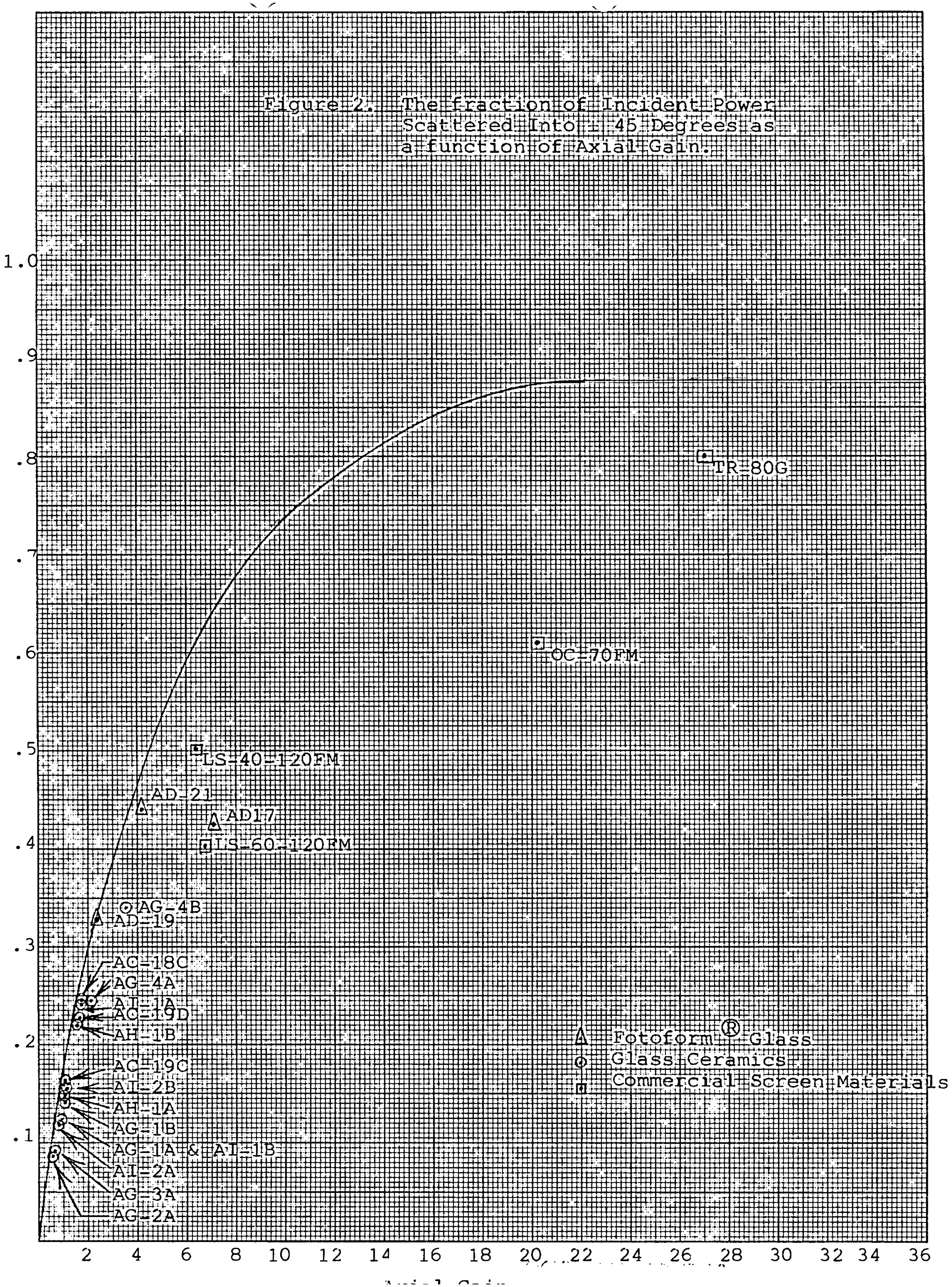

Figure 2. The fraction of Incident Power Scattered Into ± 45 Degrees as a function of Axial Gain.

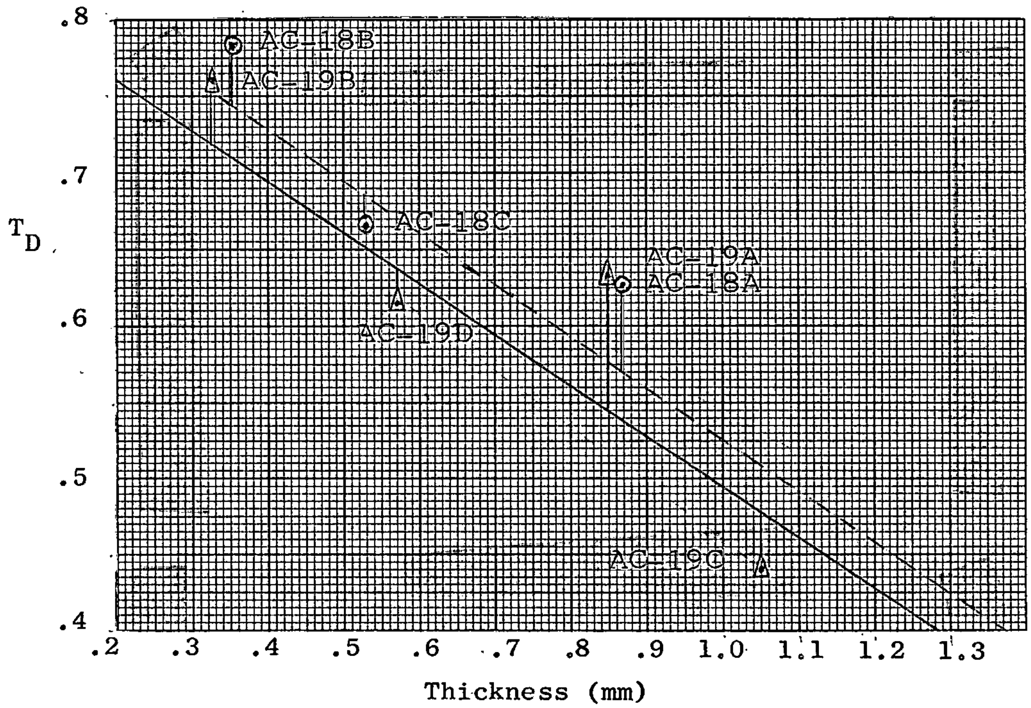

Figure 3. Diffuse Transmittance as a Function of Sample Thickness for Samples AC18 and AC19.

values of T_{spec} but still transmit some light at the red end of the spectrum. Nothing further can be accomplished by increasing the density of scattering particles because this only further reduces T_s which is already low.

We are in the process of grinding and polishing 12 new samples of material and expect 16 more within the next week. Other glass-ceramic systems as well as some containing metallic particles are being prepared.

The influence of different heat treatments can be seen from the different sizes and shapes of the crystals shown in Figure 4. The material shown is used in some of our commercial cookware. It is evident that both time and temperature are critical in determining the final crystal structure. Figures 5, 6, and 7 partially illustrate the large variety of glass-ceramic systems, each with its own particular type of crystal structure. In each of these electron photomicrographs the solid white bar represents one micron.

CRYSTALLIZATION OF A MULLITE ($3Al_2O_3 \cdot 2SiO_2$) GLASS-CERAMIC PORCELAIN

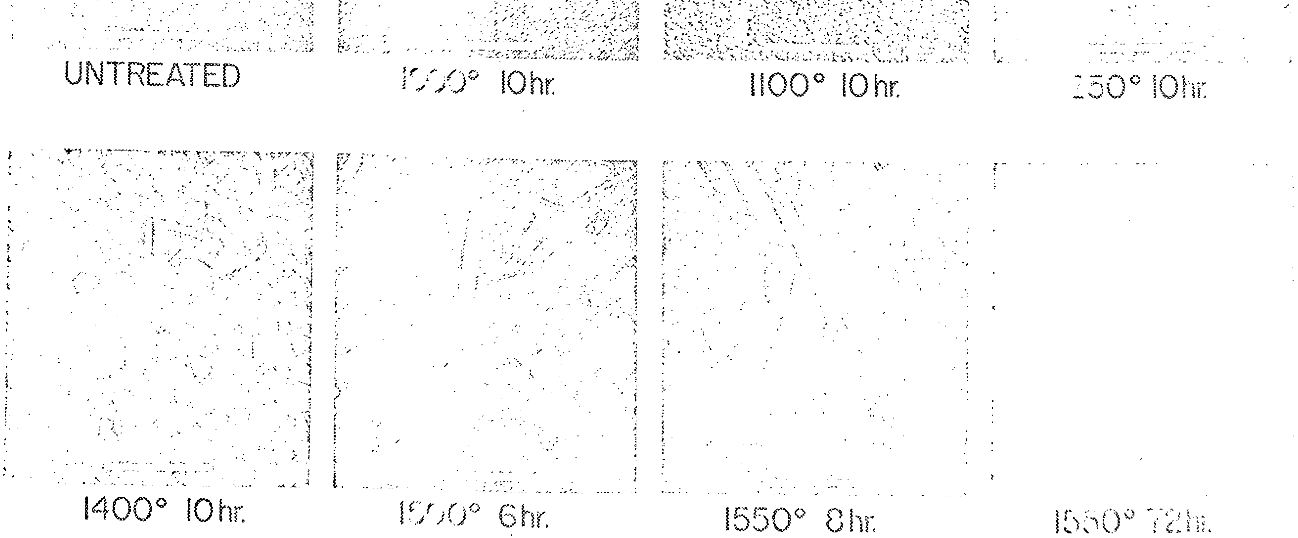

UNTREATED

1000° 10hr.

1100° 10hr.

250° 10hr.

1400° 10hr.

1500° 6hr.

1550° 8hr.

1550° 72hr.

Figure 4. Influence of the heat treatment cycle on the size and shape of the crystal system

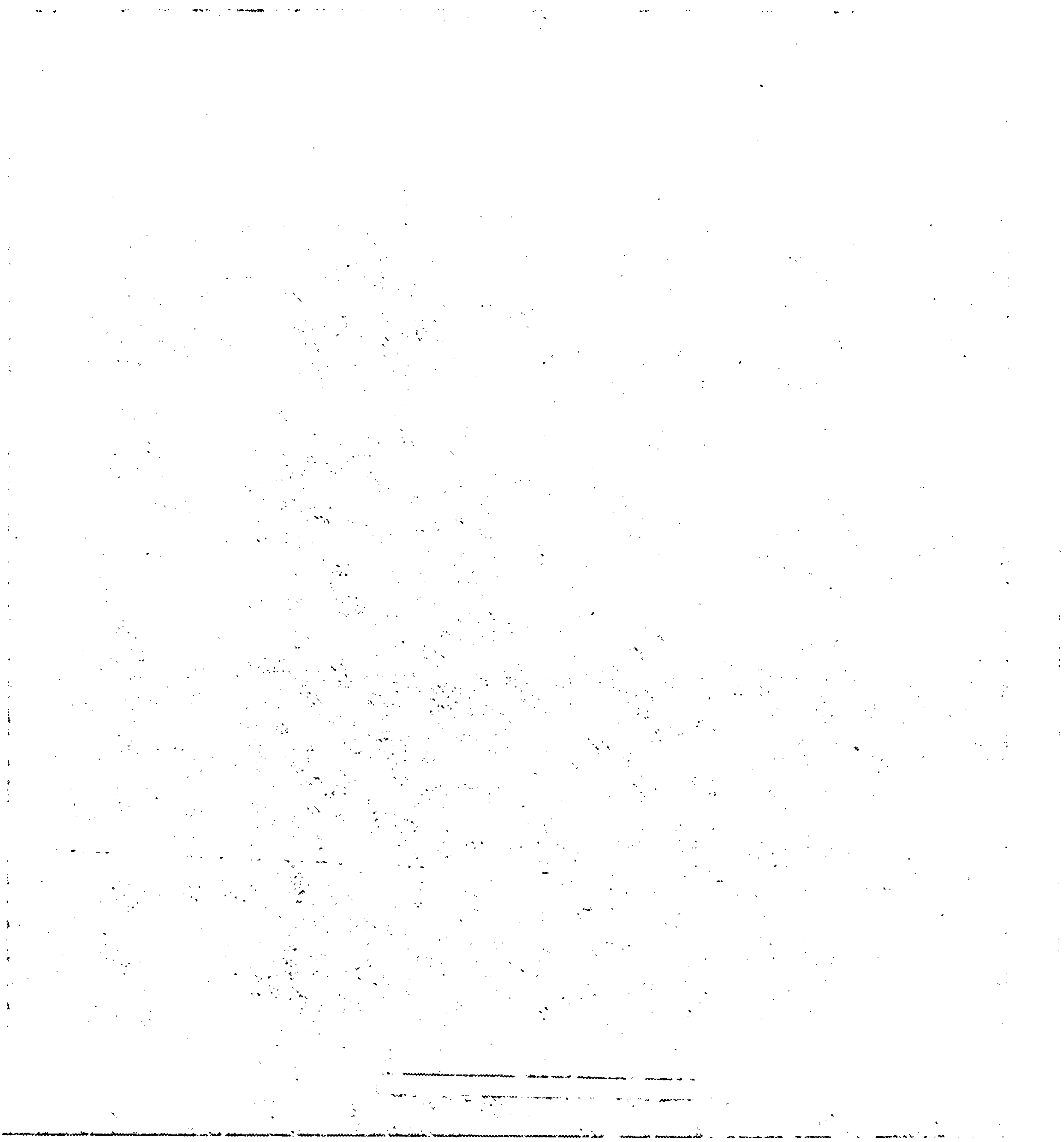

Figure 5

Figure 6. Dendritic Crystals similar to those in the samples of Fotoform® Glass.

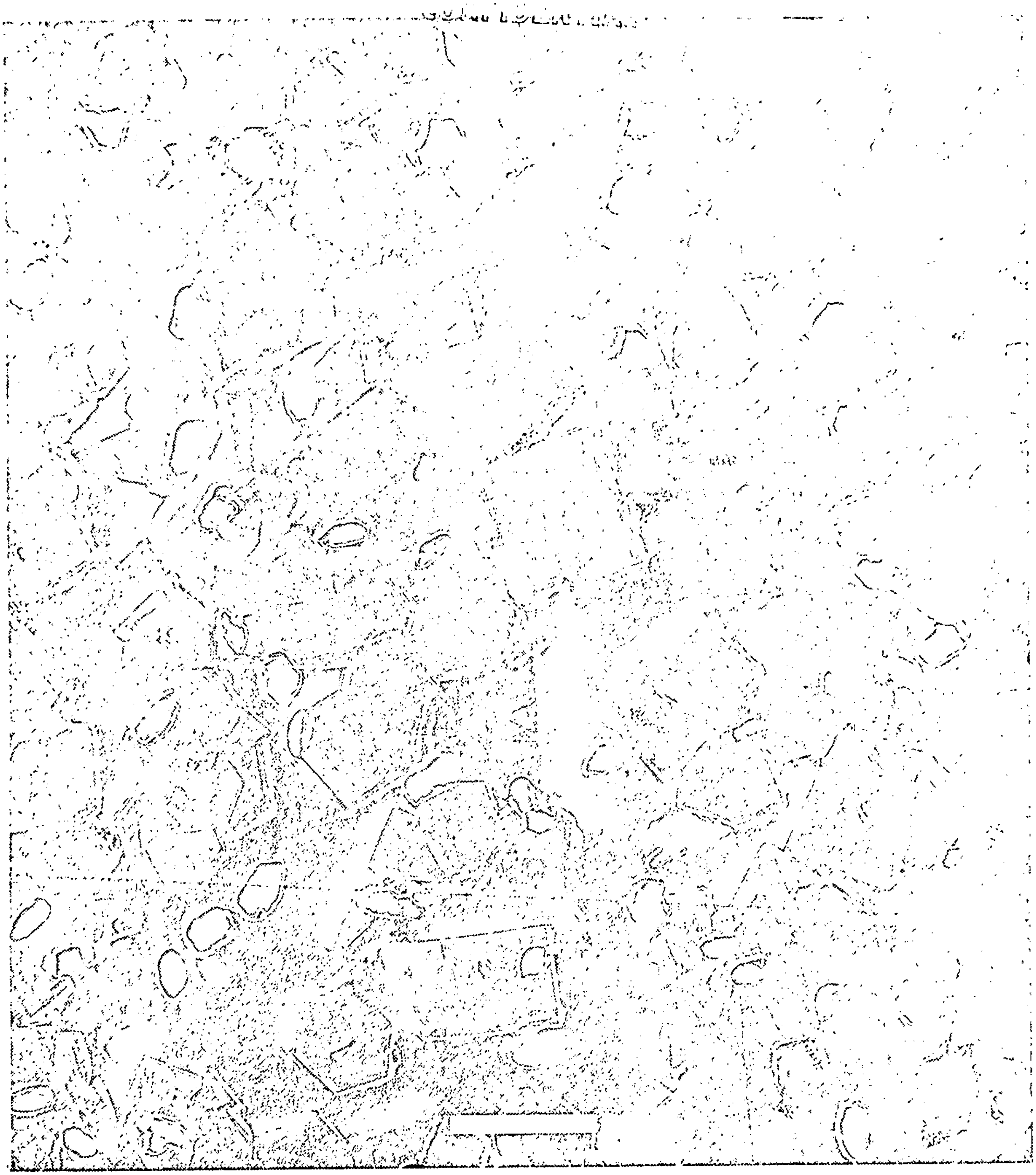

Figure 7

Our future effort with the glass-ceramic materials will consist of obtaining samples of other new systems, re-melts of those systems which look particularly promising, and re-melts of those systems which need further modification to improve their optical properties. From the re-meltings of promising systems we will fabricate small prototype screens measuring 2 to 3 inches square for further testing and evaluation. At the same time we will be investigating several different techniques of fabricating larger screens. This is important as it is almost impossible to grind screens even 6 inches square which are only one-third to one-half millimeter thick.

B. Fotoform® Glass

Fotoform® glass has many interesting properties which we are attempting to bring under control. The first of these is its ability to devitrify giving a relatively dense crystal layer over the surface of the material. We have made several samples using different heat treatments which give crystal layers from 10 to 500 microns thick. The nature of these crystals is relatively independent of the time-temperature cycle; here only the total number of crystals can be controlled. Since this layer forms only at the surface, the interior portion of the glass remains clear. This then represents a significant advantage over other materials because the thin scattering layer and the thicker structural support are an integral unit, not a thin scattering layer attached to some supporting material.

As can be seen from Figures 1 and 2, some materials have excellent transmission properties which have been verified in a rear projection system. The best of these samples, AD21, transmits over 90% of the incident light which makes it relatively insensitive to ambient illumination while differing in brightness by ±28% within a viewing angle of ±45°. Unfortunately there is some micro structure in these materials when viewed under 10x magnification. This will be investigated further to determine its exact origin. In addition, we are in the process of fabricating prototype rear projection screens from this material which are three inches square and cover a wide range of optical properties.

This glass has the additional property of being light sensitive. By exposing the desired pattern into the glass, developing it through a heat treatment, and then etching away part of the exposed area we can form lenticular elements on its surface. The resulting crystal structure of the exposed areas is similar to that of Figure 6. For our initial exposures we used two different nickel masks both 12.5 microns thick. One had 6 micron square holes with a 6 micron spacing; the second had 25 micron square holes spaced 6 microns apart, Figure 8. These masks were contacted to the Fotoform® glass between a thin sheet of borosilicate glass to give square, exposed areas. These samples were then etched giving a material with negative lenticules. Since all of the glass is actually etched and only the difference in the etch rate cuts the patterns into the glass, it was hoped we could polish the material after etching and place it back in the oven at a sufficiently high temperature so that the surface tension of the molten glass would form the clear, flat, raised sections into curved, lenticular shapes. Unfortunately, during this heating operation crystallization occurred throughout the glass producing a dense white scattering material. We are continuing our investigations of the optical properties of the lenticular configuration,

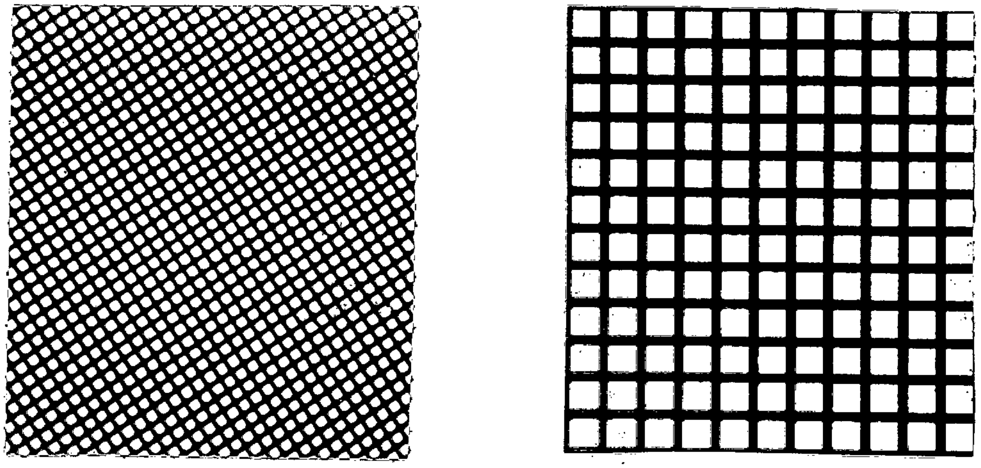

Figure 8. Micrographs of the Masks Used to Expose the Lenticular Pattern into the Fotoform® Glass.

and at the same time we are forming positive lenticules by evaporating on glass a negative of the mask previously described by following these fabrication procedures. Because of the large apparent size of the crystals in the heat-treated lenticular material, we will also be preparing samples of this and investigating the associated optical properties.

C. Lenticular Screens

1. Glass Beads

We have fabricated some small lenticular screens to gain a better understanding of their light scattering properties. These were made by covering a thin layer of a quick setting plastic with a layer of spherical glass beads before it became completely solid. After the plastic had hardened, the loose beads were removed. Screens made in this way have values of T_s from 60% to 95% depending on the size of the beads used. For our studies the bead diameter varied from 460 microns down to 75 microns. The larger beads gave very high gain, poor quality screens as expected; however, the smallest sizes gave no noticable distortion of the image as viewed directly by the eye. Naturally, under 10x magnification the beaded structure could easily be seen. Our future effort in this area will be concerned with making uniform single layers of glass beads with diameters as small as 15 to 20 microns.

2. Cylindrical Lenticules

The glass blank containing the cylindrical prism is presently being redrawn into ribbon. Figure 9 shows a end view of the original plate; actual size. We will be reporting on this in detail in the next report.

II. Instrumentation (MTF Analyzer)

The MTF Analyzer is nearing completion. Figure 10 shows a photograph of the film transport, light source and the contrast computer. The system is operated in the following way to obtain a transfer function:

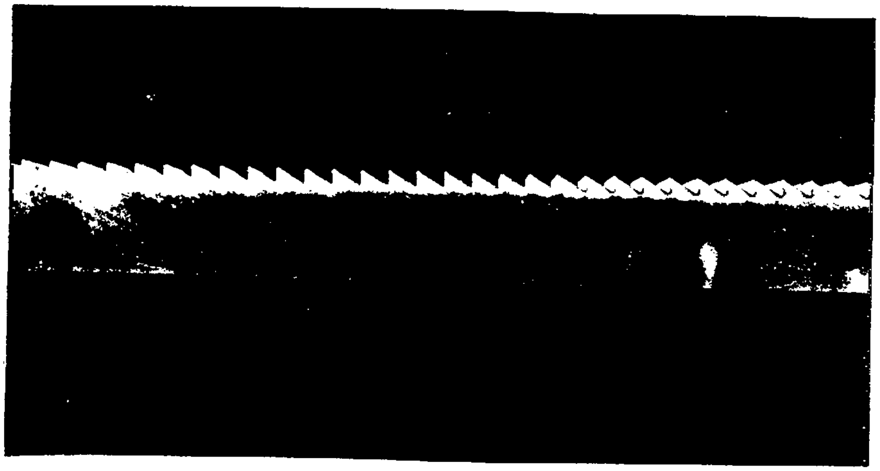

Figure 9. Cross Sectional View of Lenticular Blank

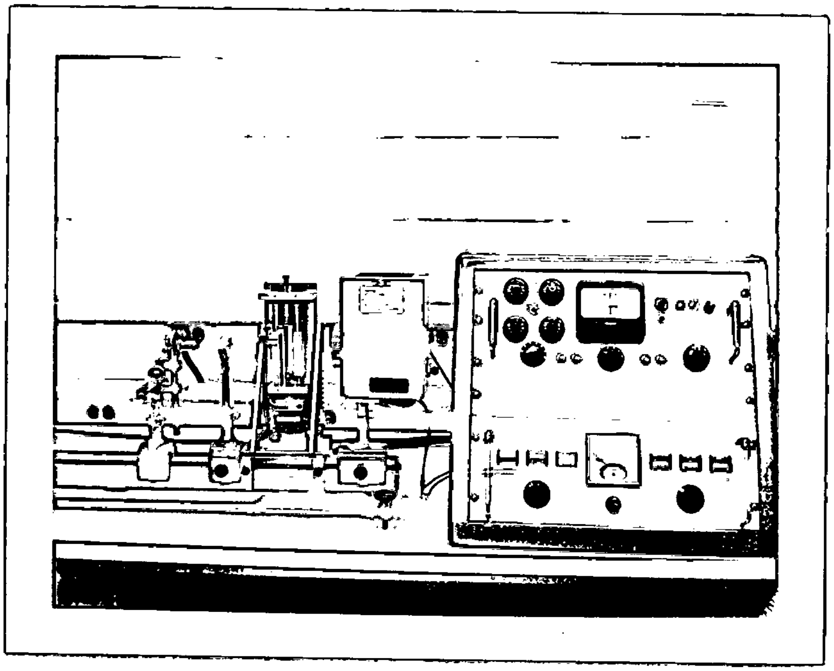

Figure 10. Photograph of our MTF Analyzer Showing the Film Transport, Light Source and Contrast Computer.

1. A sine-wave mask in the film transport is focused onto the pinhole aperture ahead of the PM tube.

2. The transport is then manually positioned at the low spatial frequency end so that a low density region of the sine-wave mask falls on the pinhole aperture. The output from the PM tube is presented to the MTF input. This signal is amplified, if necessary, by a pre-amplifier stage and then compared to an external voltage. The external voltage source is then adjusted using the "mask maximum" adjustment to null out the input signal.

3. The transport is now manually set to a high density area of the sine-wave mask and the input signal is adjusted as outlined in paragraph 2, with the exception that no additional compensation is made in the pre-amplifier. The "mask minimum" adjustment control is used to null out the PM tube output signal.

4. The sum of the voltage levels from the maximum and minimum circuits is fed into an averaging amplifier. The transport is then activated so that it traverses the full length of the strip starting at the high spatial frequency end at a varying rate. This generates a fixed frequency of 27.4 cycles/second.

   The 27.4 cycle output is summed with the output from the averaging amplifier, and the signal is again amplified and fed through a step-up transformer. The transformer output is rectified and filtered, and the resulting envelope of the AC power contained in the mask as a function of spatial frequency is fed to an x-y plotter.

5. The test procedure, when a glass sample is used, is the same as outlined in paragraphs 1-4 except now the "sample maximum" and "sample minimum" level adjustments are used. In this stage, due to the decreased voltage level as a result of the attenuating characteristics of the glass, the output from the averaging amplifier is passed through an adjustable gain amplifier to insure that the DC levels with and without the sine-wave mask are the same. The only difference is the AC signal level is a measure of the MTF of the sample. This output results in a second trace on the x-y recorder. The ratio of these then constitutes the MTF of the sample.

Data Appendix

CONFIDENTIAL

9

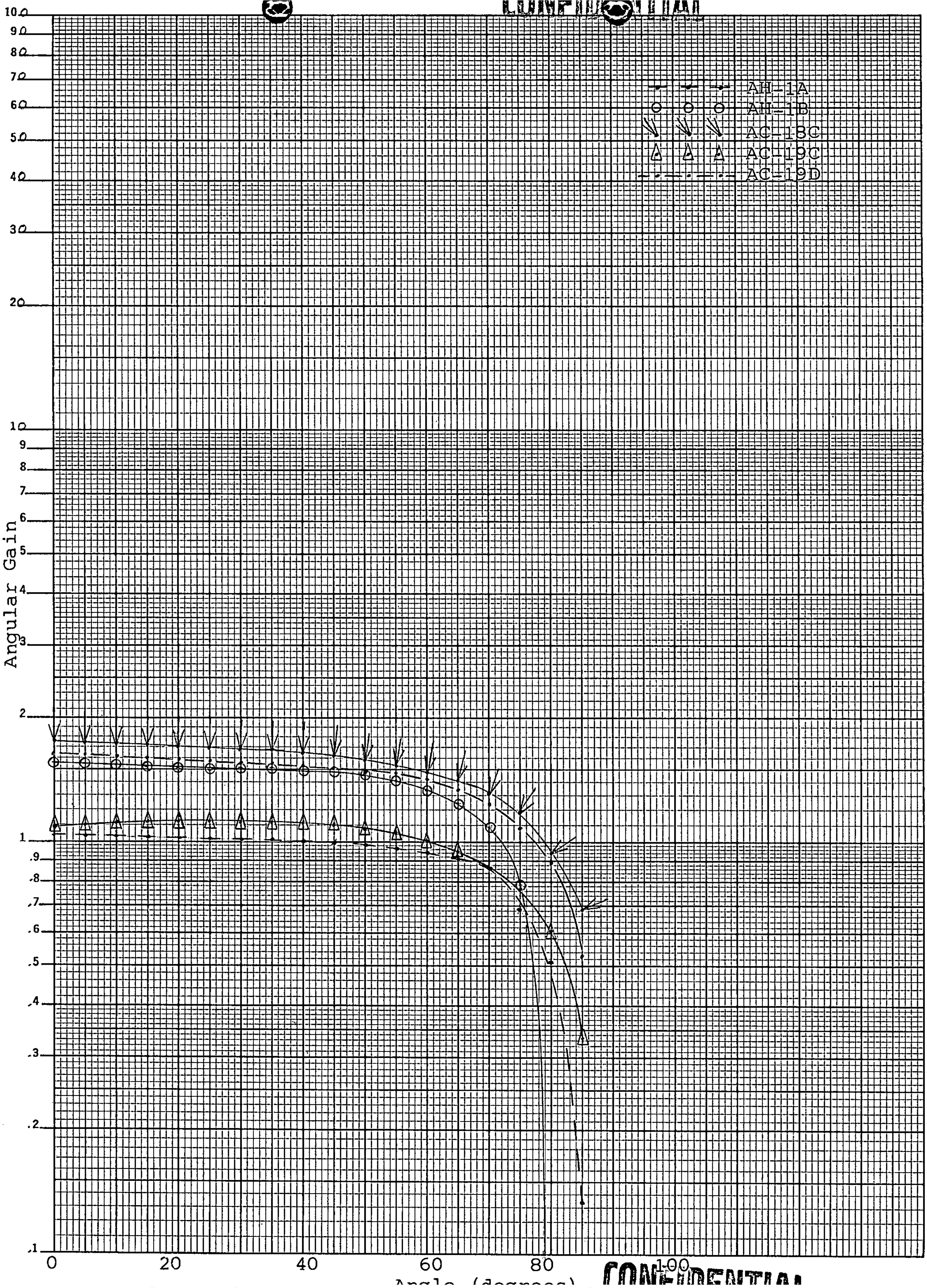

CONFIDENTIAL

CONFIDENTIAL

5

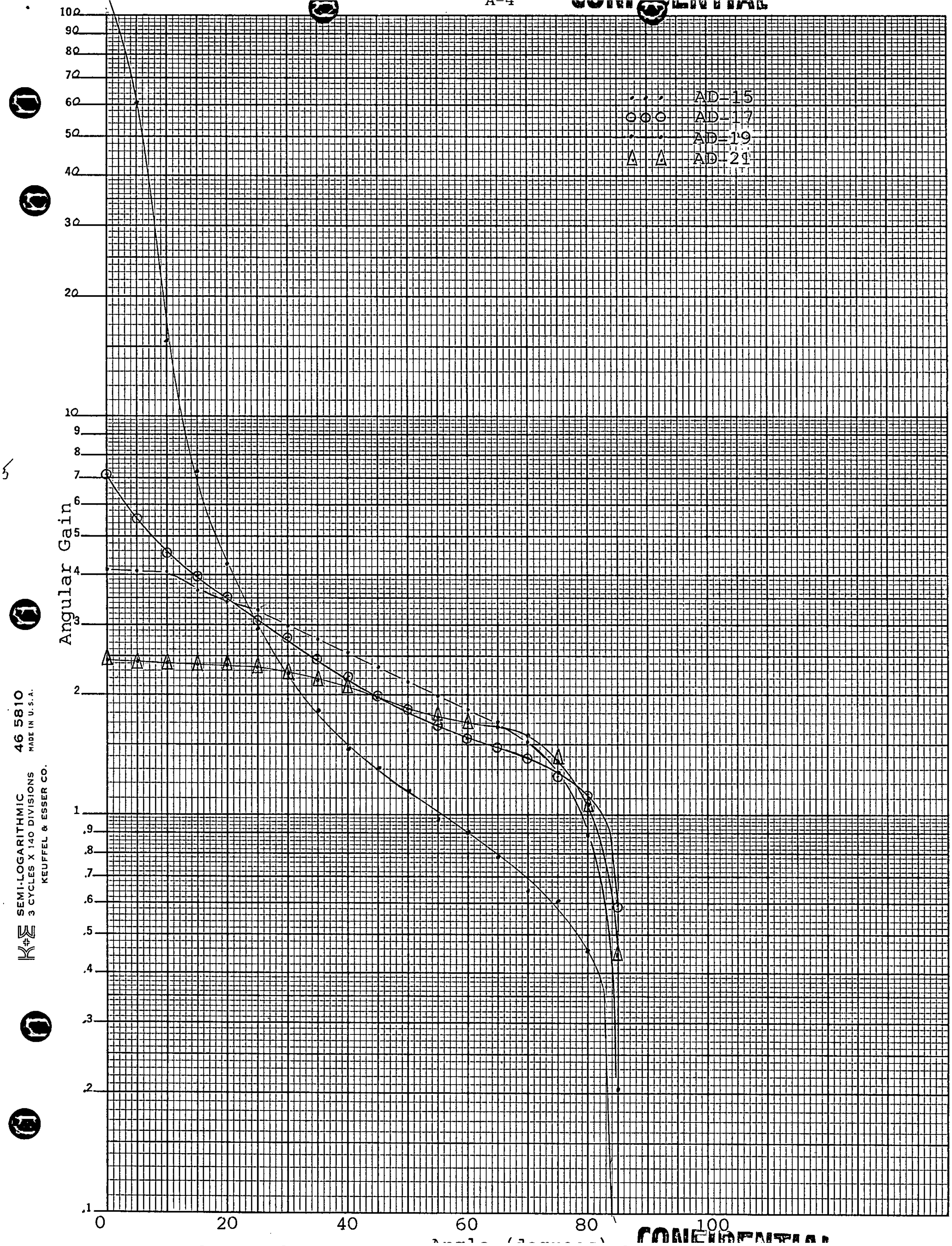

CONFIDENTIAL

CONFIDENTIAL

①

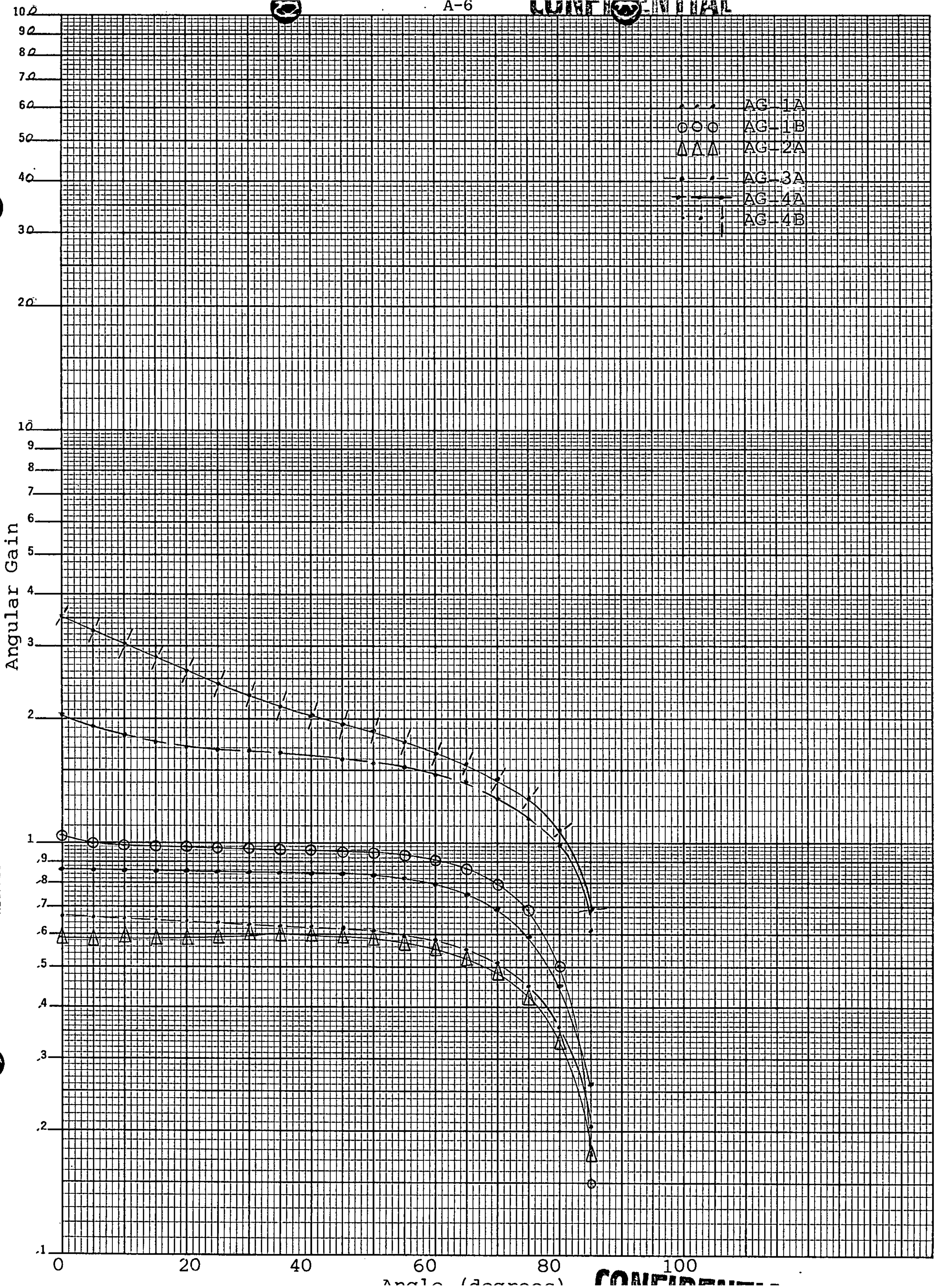

CONFIDENTIAL

CONFIDENTIAL

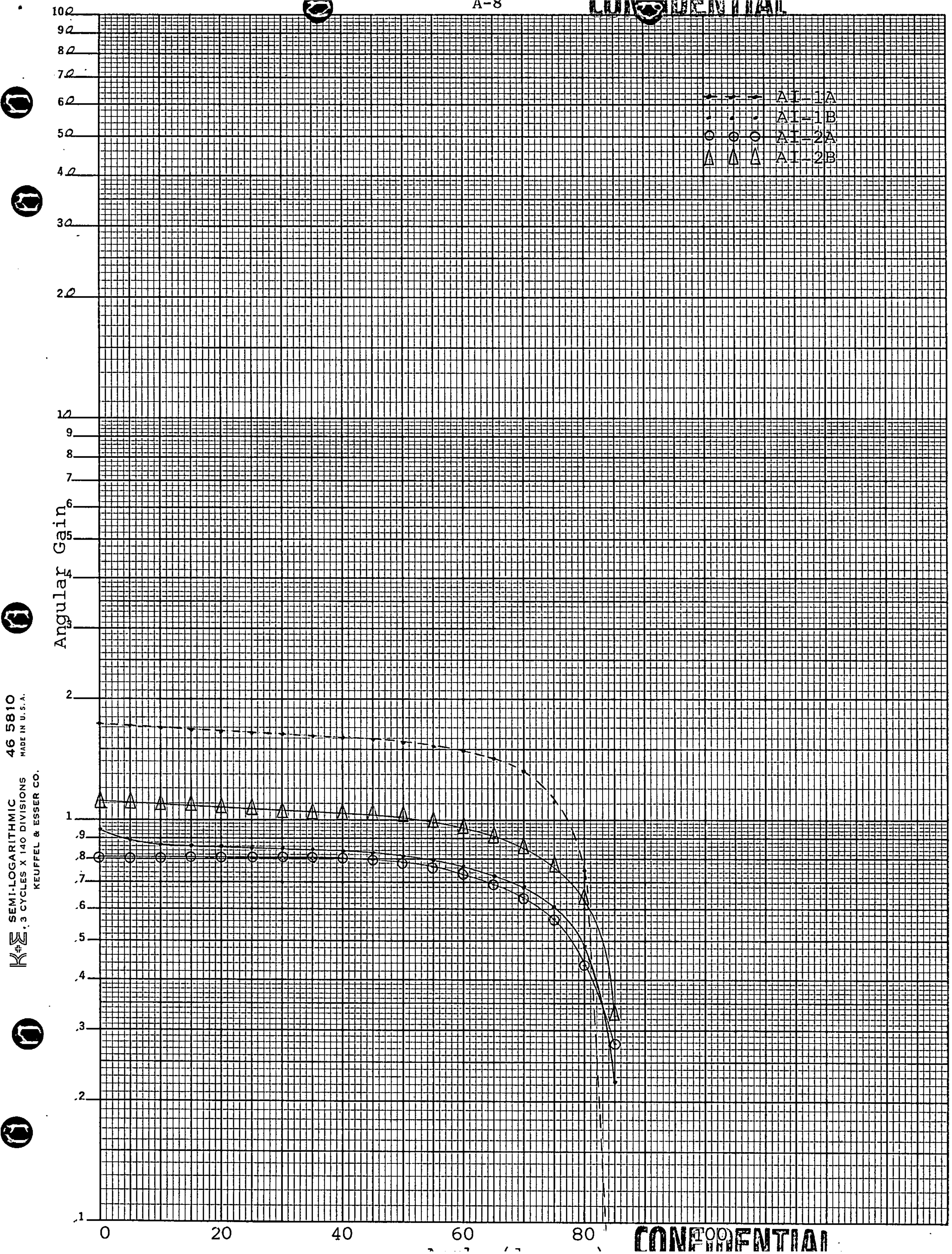

CONFIDENTIAL

③

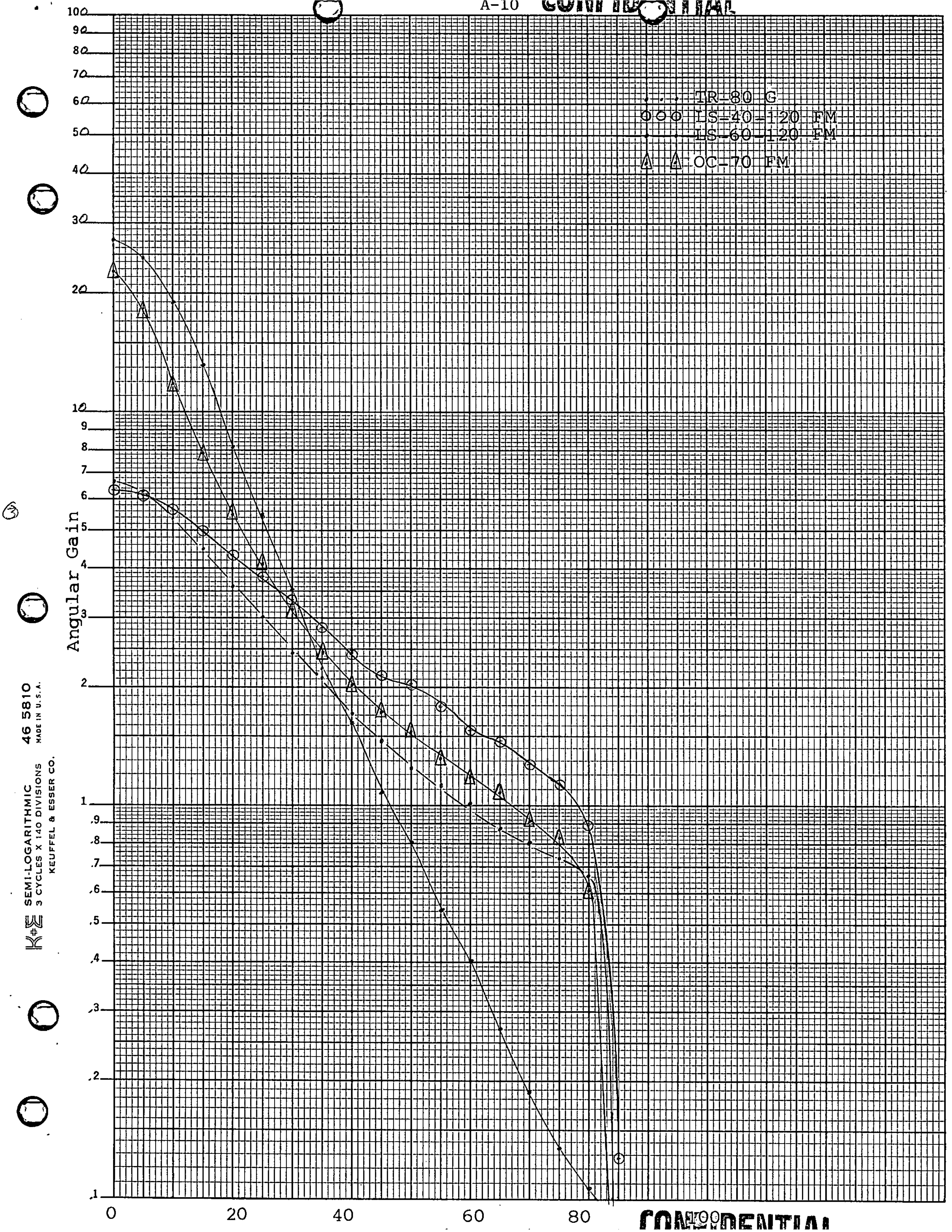

TR-80 G
LS-40-120 FM
LS-60-120 FM
OC-70 FM
Angular Gain
100
90
80
70
60
50
40
30
20
10
9
8
7
6
5
4
3
2
1
.9
.8
.7
.6
.5
.4
.3
.2
.1
0
20
40
60
80
100
K+E SEMI-LOGARITHMIC 46 5810
3 CYCLES X 140 DIVISIONS MADE IN U.S.A.
KEUFFEL & ESSER CO.